PHYSICAL REVIEW D **79,** 051102(R) (2009)

# Evidence for $B^+ \to \bar{K}^{*0} K^{*+}$

B. Aubert,[1] M. Bona,[1] Y. Karyotakis,[1] J. P. Lees,[1] V. Poireau,[1] E. Prencipe,[1] X. Prudent,[1] V. Tisserand,[1] J. Garra Tico,[2] E. Grauges,[2] L. Lopez,[3a,3b] A. Palano,[3a,3b] M. Pappagallo,[3a,3b] G. Eigen,[4] B. Stugu,[4] L. Sun,[4] M. Battaglia,[5] D. N. Brown,[5] L. T. Kerth,[5] Yu. G. Kolomensky,[5] G. Lynch,[5] I. L. Osipenkov,[5] K. Tackmann,[5] T. Tanabe,[5] C. M. Hawkes,[6] N. Soni,[6] A. T. Watson,[6] H. Koch,[7] T. Schroeder,[7] D. J. Asgeirsson,[8] B. G. Fulsom,[8] C. Hearty,[8] T. S. Mattison,[8] J. A. McKenna,[8] M. Barrett,[9] A. Khan,[9] A. Randle-Conde,[9] V. E. Blinov,[10] A. D. Bukin,[10] A. R. Buzykaev,[10] V. P. Druzhinin,[10] V. B. Golubev,[10] A. P. Onuchin,[10] S. I. Serednyakov,[10] Yu. I. Skovpen,[10] E. P. Solodov,[10] K. Yu. Todyshev,[10] M. Bondioli,[11] S. Curry,[11] I. Eschrich,[11] D. Kirkby,[11] A. J. Lankford,[11] P. Lund,[11] M. Mandelkern,[11] E. C. Martin,[11] D. P. Stoker,[11] S. Abachi,[12] C. Buchanan,[12] H. Atmacan,[13] J. W. Gary,[13] F. Liu,[13] O. Long,[13] G. M. Vitug,[13] Z. Yasin,[13] L. Zhang,[13] V. Sharma,[14] C. Campagnari,[15] T. M. Hong,[15] D. Kovalskyi,[15] M. A. Mazur,[15] J. D. Richman,[15] T. W. Beck,[16] A. M. Eisner,[16] C. A. Heusch,[16] J. Kroseberg,[16] W. S. Lockman,[16] A. J. Martinez,[16] T. Schalk,[16] B. A. Schumm,[16] A. Seiden,[16] L. O. Winstrom,[16] C. H. Cheng,[17] D. A. Doll,[17] B. Echenard,[17] F. Fang,[17] D. G. Hitlin,[17] I. Narsky,[17] T. Piatenko,[17] F. C. Porter,[17] R. Andreassen,[18] G. Mancinelli,[18] B. T. Meadows,[18] K. Mishra,[18] M. D. Sokoloff,[18] P. C. Bloom,[19] W. T. Ford,[19] A. Gaz,[19] J. F. Hirschauer,[19] M. Nagel,[19] U. Nauenberg,[19] J. G. Smith,[19] S. R. Wagner,[19] R. Ayad,[20,*] A. Soffer,[20,†] W. H. Toki,[20] R. J. Wilson,[20] E. Feltresi,[21] A. Hauke,[21] H. Jasper,[21] M. Karbach,[21] J. Merkel,[21] A. Petzold,[21] B. Spaan,[21] K. Wacker,[21] M. J. Kobel,[22] R. Nogowski,[22] K. R. Schubert,[22] R. Schwierz,[22] A. Volk,[22] D. Bernard,[23] G. R. Bonneaud,[23] E. Latour,[23] M. Verderi,[23] P. J. Clark,[24] S. Playfer,[24] J. E. Watson,[24] M. Andreotti,[25a,25b] D. Bettoni,[25a] C. Bozzi,[25a] R. Calabrese,[25a,25b] A. Cecchi,[25a,25b] G. Cibinetto,[25a,25b] P. Franchini,[25a,25b] E. Luppi,[25a,25b] M. Negrini,[25a,25b] A. Petrella,[25a,25b] L. Piemontese,[25a] V. Santoro,[25a,25b] R. Baldini-Ferroli,[26] A. Calcaterra,[26] R. de Sangro,[26] G. Finocchiaro,[26] S. Pacetti,[26] P. Patteri,[26] I. M. Peruzzi,[26,‡] M. Piccolo,[26] M. Rama,[26] A. Zallo,[26] R. Contri,[27a,27b] M. Lo Vetere,[27a,27b] M. R. Monge,[27a,27b] S. Passaggio,[27a] C. Patrignani,[27a,27b] E. Robutti,[27a] S. Tosi,[27a,27b] K. S. Chaisanguanthum,[28] M. Morii,[28] A. Adametz,[29] J. Marks,[29] S. Schenk,[29] U. Uwer,[29] F. U. Bernlochner,[30] V. Klose,[30] H. M. Lacker,[30] D. J. Bard,[31] P. D. Dauncey,[31] M. Tibbetts,[31] P. K. Behera,[32] X. Chai,[32] M. J. Charles,[32] U. Mallik,[32] J. Cochran,[33] H. B. Crawley,[33] L. Dong,[33] W. T. Meyer,[33] S. Prell,[33] E. I. Rosenberg,[33] A. E. Rubin,[33] Y. Y. Gao,[34] A. V. Gritsan,[34] Z. J. Guo,[34] N. Arnaud,[35] J. Béquilleux,[35] A. D'Orazio,[35] M. Davier,[35] J. Firmino da Costa,[35] G. Grosdidier,[35] F. Le Diberder,[35] V. Lepeltier,[35] A. M. Lutz,[35] S. Pruvot,[35] P. Roudeau,[35] M. H. Schune,[35] J. Serrano,[35] V. Sordini,[35,§] A. Stocchi,[35] G. Wormser,[35] D. J. Lange,[36] D. M. Wright,[36] I. Bingham,[37] J. P. Burke,[37] C. A. Chavez,[37] J. R. Fry,[37] E. Gabathuler,[37] R. Gamet,[37] D. E. Hutchcroft,[37] D. J. Payne,[37] C. Touramanis,[37] A. J. Bevan,[38] C. K. Clarke,[38] F. Di Lodovico,[38] R. Sacco,[38] M. Sigamani,[38] G. Cowan,[39] S. Paramesvaran,[39] A. C. Wren,[39] D. N. Brown,[40] C. L. Davis,[40] A. G. Denig,[41] M. Fritsch,[41] W. Gradl,[42] K. E. Alwyn,[42] D. Bailey,[42] R. J. Barlow,[42] G. Jackson,[42] G. D. Lafferty,[42] T. J. West,[42] J. I. Yi,[42] J. Anderson,[43] C. Chen,[43] A. Jawahery,[43] D. A. Roberts,[43] G. Simi,[43] J. M. Tuggle,[43] C. Dallapiccola,[44] E. Salvati,[44] S. Saremi,[44] R. Cowan,[45] D. Dujmic,[45] P. H. Fisher,[45] S. W. Henderson,[45] G. Sciolla,[45] M. Spitznagel,[45] F. Taylor,[45] R. K. Yamamoto,[45] M. Zhao,[45] P. M. Patel,[46] S. H. Robertson,[46] A. Lazzaro,[47a,47b] V. Lombardo,[47a] F. Palombo,[47a,47b] J. M. Bauer,[48] L. Cremaldi,[48] R. Godang,[48,‖] R. Kroeger,[48] D. J. Summers,[48] H. W. Zhao,[48] M. Simard,[49] P. Taras,[49] H. Nicholson,[50] G. De Nardo,[51a,51b] L. Lista,[51a] D. Monorchio,[51a,51b] G. Onorato,[51a,51b] C. Sciacca,[51a,51b] G. Raven,[52] H. L. Snoek,[52] C. P. Jessop,[53] K. J. Knoepfel,[53] J. M. LoSecco,[53] W. F. Wang,[53] L. A. Corwin,[54] K. Honscheid,[54] H. Kagan,[54] R. Kass,[54] J. P. Morris,[54] A. M. Rahimi,[54] J. J. Regensburger,[54] S. J. Sekula,[54] Q. K. Wong,[54] N. L. Blount,[55] J. Brau,[55] R. Frey,[55] O. Igonkina,[55] J. A. Kolb,[55] M. Lu,[55] R. Rahmat,[55] N. B. Sinev,[55] D. Strom,[55] J. Strube,[55] E. Torrence,[55] G. Castelli,[56a,56b] N. Gagliardi,[56a,56b] M. Margoni,[56a,56b] M. Morandin,[56a] M. Posocco,[56a] M. Rotondo,[56a] F. Simonetto,[56a,56b] R. Stroili,[56a,56b] C. Voci,[56a,56b] P. del Amo Sanchez,[57] E. Ben-Haim,[57] H. Briand,[57] J. Chauveau,[57] O. Hamon,[57] Ph. Leruste,[57] J. Ocariz,[57] A. Perez,[57] J. Prendki,[57] S. Sitt,[57] L. Gladney,[58] M. Biasini,[59a,59b] E. Manoni,[59a,59b] C. Angelini,[60a,60b] G. Batignani,[60a,60b] S. Bettarini,[60a,60b] G. Calderini,[60a,60b,¶] M. Carpinelli,[60a,60b,**] A. Cervelli,[60a,60b] F. Forti,[60a,60b] M. A. Giorgi,[60a,60b] A. Lusiani,[60a,60c] G. Marchiori,[60a,60b] M. Morganti,[60a,60b] N. Neri,[60a,60b] E. Paoloni,[60a,60b] G. Rizzo,[60a,60b] J. J. Walsh,[60a] D. Lopes Pegna,[61] C. Lu,[61] J. Olsen,[61] A. J. S. Smith,[61] A. V. Telnov,[61] F. Anulli,[62a] E. Baracchini,[62a,62b] G. Cavoto,[62a] R. Faccini,[62a,62b] F. Ferrarotto,[62a] F. Ferroni,[62a,62b] M. Gaspero,[62a,62b] P. D. Jackson,[62a] L. Li Gioi,[62a] M. A. Mazzoni,[62a] S. Morganti,[62a] G. Piredda,[62a] F. Renga,[62a,62b] C. Voena,[62a] M. Ebert,[63] T. Hartmann,[63] H. Schröder,[63] R. Waldi,[63] T. Adye,[64] B. Franek,[64] E. O. Olaiya,[64] F. F. Wilson,[64] S. Emery,[65] L. Esteve,[65] G. Hamel de Monchenault,[65] W. Kozanecki,[65] G. Vasseur,[65] Ch. Yèche,[65] M. Zito,[65] X. R. Chen,[66] H. Liu,[66] W. Park,[66] M. V. Purohit,[66] R. M. White,[66] J. R. Wilson,[66] M. T. Allen,[67] D. Aston,[67] R. Bartoldus,[67] J. F. Benitez,[67] R. Cenci,[67] J. P. Coleman,[67] M. R. Convery,[67] J. C. Dingfelder,[67] J. Dorfan,[67]

 

G. P. Dubois-Felsmann,[67] W. Dunwoodie,[67] R. C. Field,[67] A. M. Gabareen,[67] M. T. Graham,[67] P. Grenier,[67] C. Hast,[67] W. R. Innes,[67] J. Kaminski,[67] M. H. Kelsey,[67] H. Kim,[67] P. Kim,[67] M. L. Kocian,[67] D. W. G. S. Leith,[67] S. Li,[67] B. Lindquist,[67] S. Luitz,[67] V. Luth,[67] H. L. Lynch,[67] D. B. MacFarlane,[67] H. Marsiske,[67] R. Messner,[67] D. R. Muller,[67] H. Neal,[67] S. Nelson,[67] C. P. O'Grady,[67] I. Ofte,[67] M. Perl,[67] B. N. Ratcliff,[67] A. Roodman,[67] A. A. Salnikov,[67] R. H. Schindler,[67] J. Schwiening,[67] A. Snyder,[67] D. Su,[67] M. K. Sullivan,[67] K. Suzuki,[67] S. K. Swain,[67] J. M. Thompson,[67] J. Va'vra,[67] A. P. Wagner,[67] M. Weaver,[67] C. A. West,[67] W. J. Wisniewski,[67] M. Wittgen,[67] D. H. Wright,[67] H. W. Wulsin,[67] A. K. Yarritu,[67] K. Yi,[67] C. C. Young,[67] V. Ziegler,[67] P. R. Burchat,[68] A. J. Edwards,[68] T. S. Miyashita,[68] S. Ahmed,[69] M. S. Alam,[69] J. A. Ernst,[69] B. Pan,[69] M. A. Saeed,[69] S. B. Zain,[69] S. M. Spanier,[70] B. J. Wogsland,[70] R. Eckmann,[71] J. L. Ritchie,[71] A. M. Ruland,[71] C. J. Schilling,[71] R. F. Schwitters,[71] B. W. Drummond,[72] J. M. Izen,[72] X. C. Lou,[72] F. Bianchi,[73a,73b] D. Gamba,[73a,73b] M. Pelliccioni,[73a,73b] M. Bomben,[74a,74b] L. Bosisio,[74a,74b] C. Cartaro,[74a,74b] G. Della Ricca,[74a,74b] L. Lanceri,[74a,74b] L. Vitale,[74a,74b] V. Azzolini,[75] N. Lopez-March,[75] F. Martinez-Vidal,[75] D. A. Milanes,[75] A. Oyanguren,[75] J. Albert,[76] Sw. Banerjee,[76] B. Bhuyan,[76] H. H. F. Choi,[76] K. Hamano,[76] G. J. King,[76] R. Kowalewski,[76] M. J. Lewczuk,[76] I. M. Nugent,[76] J. M. Roney,[76] R. J. Sobie,[76] T. J. Gershon,[1] P. F. Harrison,[1] J. Ilic,[1] T. E. Latham,[1] G. B. Mohanty,[1] E. M. T. Puccio,[1] H. R. Band,[78] X. Chen,[78] S. Dasu,[78] K. T. Flood,[78] Y. Pan,[78] R. Prepost,[78] C. O. Vuosalo,[78] and S. L. Wu[78]

(*BABAR* Collaboration)

[1]*Laboratoire de Physique des Particules, IN2P3/CNRS et Université de Savoie, F-74941 Annecy-Le-Vieux, France*
[2]*Universitat de Barcelona, Facultat de Fisica, Departament ECM, E-08028 Barcelona, Spain*
[3a]*INFN Sezione di Bari, I-70126 Bari, Italy;*
[3b]*Dipartmento di Fisica, Università di Bari, I-70126 Bari, Italy*
[4]*University of Bergen, Institute of Physics, N-5007 Bergen, Norway*
[5]*Lawrence Berkeley National Laboratory and University of California, Berkeley, California 94720, USA*
[6]*University of Birmingham, Birmingham B15 2TT, United Kingdom*
[7]*Ruhr Universität Bochum, Institut für Experimentalphysik 1, D-44780 Bochum, Germany*
[8]*University of British Columbia, Vancouver, British Columbia V6T 1Z1, Canada*
[9]*Brunel University, Uxbridge, Middlesex UB8 3PH, United Kingdom*
[10]*Budker Institute of Nuclear Physics, Novosibirsk 630090, Russia*
[11]*University of California at Irvine, Irvine, California 92697, USA*
[12]*University of California at Los Angeles, Los Angeles, California 90024, USA*
[13]*University of California at Riverside, Riverside, California 92521, USA*
[14]*University of California at San Diego, La Jolla, California 92093, USA*
[15]*University of California at Santa Barbara, Santa Barbara, California 93106, USA*
[16]*University of California at Santa Cruz, Institute for Particle Physics, Santa Cruz, California 95064, USA*
[17]*California Institute of Technology, Pasadena, California 91125, USA*
[18]*University of Cincinnati, Cincinnati, Ohio 45221, USA*
[19]*University of Colorado, Boulder, Colorado 80309, USA*
[20]*Colorado State University, Fort Collins, Colorado 80523, USA*
[21]*Technische Universität Dortmund, Fakultät Physik, D-44221 Dortmund, Germany*
[22]*Technische Universität Dresden, Institut für Kern- und Teilchenphysik, D-01062 Dresden, Germany*
[23]*Laboratoire Leprince-Ringuet, CNRS/IN2P3, Ecole Polytechnique, F-91128 Palaiseau, France*
[24]*University of Edinburgh, Edinburgh EH9 3JZ, United Kingdom*
[25a]*INFN Sezione di Ferrara, I-44100 Ferrara, Italy;*
[25b]*Dipartimento di Fisica, Università di Ferrara, I-44100 Ferrara, Italy*
[26]*INFN Laboratori Nazionali di Frascati, I-00044 Frascati, Italy*
[27a]*INFN Sezione di Genova, I-16146 Genova, Italy;*
[27b]*Dipartimento di Fisica, Università di Genova, I-16146 Genova, Italy*
[28]*Harvard University, Cambridge, Massachusetts 02138, USA*
[29]*Universität Heidelberg, Physikalisches Institut, Philosophenweg 12, D-69120 Heidelberg, Germany*
[30]*Humboldt-Universität zu Berlin, Institut für Physik, Newtonstr. 15, D-12489 Berlin, Germany*
[31]*Imperial College London, London SW7 2AZ, United Kingdom*
[32]*University of Iowa, Iowa City, Iowa 52242, USA*
[33]*Iowa State University, Ames, Iowa 50011-3160, USA*
[34]*Johns Hopkins University, Baltimore, Maryland 21218, USA*
[35]*Laboratoire de l'Accélérateur Linéaire, IN2P3/CNRS et Université Paris-Sud 11, Centre Scientifique d'Orsay, B. P. 34, F-91898 Orsay Cedex, France*

[36]*Lawrence Livermore National Laboratory, Livermore, California 94550, USA*
[37]*University of Liverpool, Liverpool L69 7ZE, United Kingdom*
[38]*Queen Mary, University of London, London E1 4NS, United Kingdom*
[39]*University of London, Royal Holloway and Bedford New College, Egham, Surrey TW20 0EX, United Kingdom*
[40]*University of Louisville, Louisville, Kentucky 40292, USA*
[41]*Johannes Gutenberg-Universität Mainz, Institut für Kernphysik, D-55099 Mainz, Germany*
[42]*University of Manchester, Manchester M13 9PL, United Kingdom*
[43]*University of Maryland, College Park, Maryland 20742, USA*
[44]*University of Massachusetts, Amherst, Massachusetts 01003, USA*
[45]*Massachusetts Institute of Technology, Laboratory for Nuclear Science, Cambridge, Massachusetts 02139, USA*
[46]*McGill University, Montréal, Québec H3A 2T8, Canada*
[47a]*INFN Sezione di Milano, I-20133 Milano, Italy;*
[47b]*Dipartimento di Fisica, Università di Milano, I-20133 Milano, Italy*
[48]*University of Mississippi, University, Mississippi 38677, USA*
[49]*Université de Montréal, Physique des Particules, Montréal, Québec H3C 3J7, Canada*
[50]*Mount Holyoke College, South Hadley, Massachusetts 01075, USA*
[51a]*INFN Sezione di Napoli, I-80126 Napoli, Italy;*
[51b]*Dipartimento di Scienze Fisiche, Università di Napoli Federico II, I-80126 Napoli, Italy*
[52]*NIKHEF, National Institute for Nuclear Physics and High Energy Physics, NL-1009 DB Amsterdam, The Netherlands*
[53]*University of Notre Dame, Notre Dame, Indiana 46556, USA*
[54]*Ohio State University, Columbus, Ohio 43210, USA*
[55]*University of Oregon, Eugene, Oregon 97403, USA*
[56a]*INFN Sezione di Padova, I-35131 Padova, Italy;*
[56b]*Dipartimento di Fisica, Università di Padova, I-35131 Padova, Italy*
[57]*Laboratoire de Physique Nucléaire et de Hautes Energies, IN2P3/CNRS, Université Pierre et Marie Curie-Paris6, Université Denis Diderot-Paris7, F-75252 Paris, France*
[58]*University of Pennsylvania, Philadelphia, Pennsylvania 19104, USA*
[59a]*INFN Sezione di Perugia, I-06100 Perugia, Italy;*
[59b]*Dipartimento di Fisica, Università di Perugia, I-06100 Perugia, Italy*
[60a]*INFN Sezione di Pisa, I-56127 Pisa, Italy;*
[60b]*Dipartimento di Fisica, Università di Pisa, I-56127 Pisa, Italy;*
[60c]*Scuola Normale Superiore di Pisa, I-56127 Pisa, Italy*
[61]*Princeton University, Princeton, New Jersey 08544, USA*
[62a]*INFN Sezione di Roma, I-00185 Roma, Italy;*
[62b]*Dipartimento di Fisica, Università di Roma La Sapienza, I-00185 Roma, Italy*
[63]*Universität Rostock, D-18051 Rostock, Germany*
[64]*Rutherford Appleton Laboratory, Chilton, Didcot, Oxon OX11 0QX, United Kingdom*
[65]*CEA, Irfu, SPP, Centre de Saclay, F-91191 Gif-sur-Yvette, France*
[66]*University of South Carolina, Columbia, South Carolina 29208, USA*
[67]*SLAC National Accelerator Laboratory, Stanford, California 94309, USA*
[68]*Stanford University, Stanford, California 94305-4060, USA*
[69]*State University of New York, Albany, New York 12222, USA*
[70]*University of Tennessee, Knoxville, Tennessee 37996, USA*
[71]*University of Texas at Austin, Austin, Texas 78712, USA*
[72]*University of Texas at Dallas, Richardson, Texas 75083, USA*
[73a]*INFN Sezione di Torino, I-10125 Torino, Italy;*
[73b]*Dipartimento di Fisica Sperimentale, Università di Torino, I-10125 Torino, Italy*
[74a]*INFN Sezione di Trieste, I-34127 Trieste, Italy;*
[74b]*Dipartimento di Fisica, Università di Trieste, I-34127 Trieste, Italy*
[75]*IFIC, Universitat de Valencia-CSIC, E-46071 Valencia, Spain*
[76]*University of Victoria, Victoria, British Columbia V8W 3P6, Canada*
[1]*Department of Physics, University of Warwick, Coventry CV4 7AL, United Kingdom*

[*]Now at Temple University, Philadelphia, PA 19122, USA.
[†]Now at Tel Aviv University, Tel Aviv, 69978, Israel.
[‡]Also at Università di Perugia, Dipartimento di Fisica, Perugia, Italy.
[§]Also at Università di Roma La Sapienza, I-00185 Roma, Italy.
[‖]Now at University of South Alabama, Mobile, AL 36688, USA.
[¶]Also at Laboratoire de Physique Nucléaire et de Hautes Energies, IN2P3/CNRS, Université Pierre et Marie Curie-Paris6, Université Denis Diderot-Paris7, F-75252 Paris, France.
[**]Also at Università di Sassari, Sassari, Italy.

[78]*University of Wisconsin, Madison, Wisconsin 53706, USA*

(Received 12 January 2009; published 19 March 2009)

We present measurements of the branching fraction and fraction of longitudinal polarization for the decay $B^+ \to \bar{K}^{*0}K^{*+}$ with a sample of $(467 \pm 5) \times 10^6$ $B\bar{B}$ pairs collected with the *BABAR* detector at the PEP-II asymmetric-energy $e^+e^-$ collider at the SLAC National Accelerator Laboratory. We obtain the branching fraction $\mathcal{B}(B^+ \to \bar{K}^{*0}K^{*+}) = (1.2 \pm 0.5 \pm 0.1) \times 10^{-6}$ with a significance of 3.7 standard deviations including systematic uncertainties. We measure the fraction of longitudinal polarization $f_L = 0.75^{+0.16}_{-0.26} \pm 0.03$. The first error quoted is statistical and the second is systematic.

DOI: 10.1103/PhysRevD.79.051102 PACS numbers: 13.25.Hw, 11.30.Er, 12.15.Hh

The study of the branching fractions and angular distributions of $B$ meson decays to hadronic final states without a charm quark probes the dynamics of both the weak and strong interactions, and plays an important role in understanding $CP$ violation in the quark sector. Improved experimental measurements of these charmless decays, combined with theoretical developments, can provide significant constraints on the Cabibbo-Kobayashi-Maskawa (CKM) matrix parameters [1] and uncover evidence for physics beyond the standard model [2,3].

QCD factorization models predict the fraction of longitudinal polarization $f_L$ of the decay of the $B$ meson to two vector particles ($VV$) to be ~0.9 for both tree- and loop-dominated (penguin) decays [4]. However, measurements of the penguin $VV$ decays $B^+ \to \phi K^{*+}$ and $B^0 \to \phi K^{*0}$ give $f_L$ approximately 0.5 [5], while $f_L = 0.81^{+0.10}_{-0.12} \pm 0.06$ has been measured for the decay $B^0 \to K^{*0}\bar{K}^{*0}$ [6]. Several attempts to understand the values of $f_L$ within or beyond the standard model have been made [7]. Further information about decays related by $SU(3)$ symmetry may provide insights into this polarization discrepancy and test possible modifications to factorization models, such as penguin annihilation or rescattering [8].

A number of papers have calculated the expected branching fractions for the decay of a $B$ meson to $VV$ final states, including $B^0 \to K^{*+}K^{*-}$, $B^0 \to K^{*0}\bar{K}^{*0}$, and $B^+ \to \bar{K}^{*0}K^{*+}$. The decay $B^+ \to \bar{K}^{*0}K^{*+}$, like $B^0 \to K^{*0}\bar{K}^{*0}$, occurs through both electroweak and gluonic $b \to d$ penguin loops, as shown in Fig. 1, while the decay $B^0 \to K^{*+}K^{*-}$ proceeds through a $b \to u$ quark transition via $W$ exchange. The $B^+ \to \bar{K}^{*0}K^{*+}$ branching fraction is expected to be of the same order as $B^0 \to K^{*0}\bar{K}^{*0}$, with Beneke, Rohrer, and Yang [2] predicting $(0.5^{+0.2+0.4}_{-0.1-0.3}) \times 10^{-6}$, while Cheng and Yang [3] quote $(0.6 \pm 0.1 \pm 0.3) \times 10^{-6}$, both based on QCD factorization. The $B^0 \to K^{*0}\bar{K}^{*0}$ branching fraction has been measured to be $(1.28^{+0.35}_{-0.30} \pm 0.11) \times 10^{-6}$ [6], where the first error is statistical and the second systematic, while an upper limit at the 90% confidence level (C.L.) of $2.0 \times 10^{-6}$ has been recently placed on the $B^0 \to K^{*-}K^{*+}$ branching fraction [9]. The current experimental upper limit on the $B^+ \to \bar{K}^{*0}K^{*+}$ branching fraction at the 90% C.L. is $71(48) \times 10^{-6}$ [10], assuming a fully longitudinally (transversely) polarized system.

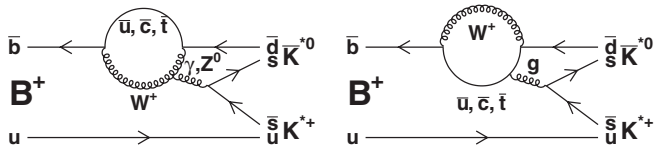


FIG. 1. The electroweak (left panel) and gluonic (right panel) $b \to d$ penguin loop diagrams for $B^+ \to \bar{K}^{*0}K^{*+}$.

We report on a search for the decay mode $B^+ \to \bar{K}^{*0}K^{*+}$, where $K^*$ refers to the $K^*(892)$ resonance, with consideration of nonresonant backgrounds [11]. The analysis is based on a data sample of $(467 \pm 5) \times 10^6$ $B\bar{B}$ pairs, corresponding to an integrated luminosity of 426 fb$^{-1}$, collected with the *BABAR* detector at the PEP-II asymmetric-energy $e^+e^-$ collider operated at the SLAC National Accelerator Laboratory. The $e^+e^-$ center-of-mass (c.m.) energy is $\sqrt{s} = 10.58$ GeV, corresponding to the $\Upsilon(4S)$ resonance mass (on-resonance data). In addition, 44.4 fb$^{-1}$ of data collected 40 MeV below the $\Upsilon(4S)$ resonance (off-resonance data) are used for background studies. We assume equal production rates of $B^+B^-$ and $B^0\bar{B}^0$ mesons.

The *BABAR* detector is described in detail in Ref. [12]. Charged particles are reconstructed as tracks with a five-layer silicon vertex detector and a 40-layer drift chamber inside a 1.5 T solenoidal magnet. An electromagnetic calorimeter (EMC) comprised of 6580 CsI(Tl) crystals is used to identify electrons and photons. A ring-imaging Cherenkov detector (DIRC) is used to identify charged hadrons and to provide additional electron identification information. The average $K$-$\pi$ separation in the DIRC varies from $12\sigma$ at a laboratory momentum of 1.5 GeV/$c$ to $2.5\sigma$ at 4.5 GeV/$c$. Muons are identified by an instrumented magnetic-flux return (IFR).

The $B^+ \to \bar{K}^{*0}K^{*+}$ candidates are reconstructed through the decays of $\bar{K}^{*0} \to K^-\pi^+$ and $K^{*+} \to K^0_S\pi^+$ or $K^{*+} \to K^+\pi^0$, with $K^0_S \to \pi^+\pi^-$ and $\pi^0 \to \gamma\gamma$. The differential decay rate, after integrating over the angle between the decay planes of the vector mesons, for which the acceptance is nearly uniform, is

$$\frac{1}{\Gamma}\frac{d^2\Gamma}{d\cos\theta_1 d\cos\theta_2} \propto \frac{1-f_L}{4}\sin^2\theta_1\sin^2\theta_2 + f_L\cos^2\theta_1\cos^2\theta_2, \quad (1)$$

where $\theta_1$ and $\theta_2$ are the helicity angles of the $K^{*+}$ and $\bar{K}^{*0}$, defined as the angle between the daughter kaon ($K^0_S$ or $K^\pm$) momentum and the direction opposite to the $B$ meson in the $K^*$ rest frame [13].

The charged particles from the $K^*$ decays are required to have a transverse momentum relative to the beam axis greater than 0.05 GeV/$c$. The particles are identified as either charged pions or kaons by measurement of the energy loss in the tracking devices, the number of photons recorded by the DIRC, and the corresponding Cherenkov angle. These measurements are combined with additional information from the EMC and IFR detectors, where appropriate, to reject electrons, muons, and protons.

The $K^0_S$ candidates are required to have a mass within 0.01 GeV/$c^2$ of the nominal $K^0_S$ mass [14], a decay vertex separated from the $B$ meson decay vertex by at least 20 times the uncertainty in the measurement of the separation of the vertex positions, a flight distance in the direction transverse to the beam axis of at least 0.3 cm, and the cosine of the angle between the line joining the $B$ and $K^0_S$ decay vertices and the $K^0_S$ momentum greater than 0.999.

In the laboratory frame, the energy of each photon from the $\pi^0$ candidate must be greater than 0.04 GeV, the energy of the $\pi^0$ must exceed 0.25 GeV, and the reconstructed $\pi^0$ invariant mass is required to be in the range $0.12 \leq m_{\gamma\gamma} \leq 0.15$ GeV/$c^2$. After selection, the $\pi^0$ candidate's mass is constrained to its nominal value [14].

We require the invariant mass of the $K^*$ candidates to satisfy $0.792 < m_{K\pi} < 0.992$ GeV/$c^2$. A $B$ meson candidate is formed from the $\bar{K}^{*0}$ and $K^{*+}$ candidates, with the condition that the $K^*$ candidates originate from the interaction region and the $\chi^2$ of the $B$ meson vertex fit is less than 100. A second $B$ meson is formed by creating a vertex from the remaining tracks, with the condition that they are consistent with originating from the interaction region and at least one of the tracks is charged [15].

The $B$ meson candidates are characterized kinematically by the energy difference $\Delta E = E^*_B - \sqrt{s}/2$ and the beam energy-substituted mass $m_{\rm ES} = [(s/2 + \mathbf{p}_i \cdot \mathbf{p}_B)^2/E_i^2 - \mathbf{p}_B^2]^{1/2}$, where $(E_i, \mathbf{p}_i)$ and $(E_B, \mathbf{p}_B)$ are the four-momenta of the $\Upsilon(4S)$ and $B$ meson candidate in the laboratory frame, respectively, and the asterisk denotes the c.m. frame. The total event sample is taken from the region $-0.10 \leq \Delta E \leq 0.15$ GeV and $5.25 \leq m_{\rm ES} \leq 5.29$ GeV/$c^2$. The asymmetric $\Delta E$ criterion is applied to remove backgrounds from $B$ to charm decays that occur in the negative $\Delta E$ region; the $m_{\rm ES}$ range ensures the shape of the background distribution is properly modeled. Events outside the region $|\Delta E| \leq 0.07$ GeV and $5.27 \leq m_{\rm ES} \leq 5.29$ GeV/$c^2$ are used to characterize the background.

We suppress the background from decays to charmed states by forming the invariant mass $m_D$ from combinations of three out of the four daughter particles' four-momenta. The event is rejected if $1.845 < m_D < 1.895$ GeV/$c^2$ and the charge and particle type of the tracks are consistent with a known decay from a $D$ meson [14]. Backgrounds from $B \to \phi K^*$ are reduced by assigning the kaon mass to the pion candidate and rejecting the event if the invariant mass of the two charged tracks is between 1.00 and 1.04 GeV/$c^2$. Finally, to reduce the continuum background and to avoid the region where the reconstruction efficiency falls off rapidly for low momentum tracks, we require the cosine of the helicity angle of the $K^*$ candidates to satisfy $\cos\theta \leq 0.98$.

To reject the dominant background consisting of light-quark $q\bar{q}$ ($q = u, d, s, c$) continuum events, we require $|\cos\theta_T| < 0.8$, where $\theta_T$ is the angle, in the c.m. frame, between the thrust axis [16] of the $B$ meson and that formed from the other tracks and neutral clusters in the event. Signal events have a flat distribution in $|\cos\theta_T|$, while continuum events peak at 1.

We use Monte Carlo (MC) simulations of the signal decay to estimate the number of signal candidates per event. After the application of the selection criteria, the average number of signal candidates per event is 1.06 (1.02) for fully longitudinally (transversely) polarized decays with no $\pi^0$ in the final state and 1.15 (1.07) for decays with one $\pi^0$ in the final state. The candidate with the smallest fitted decay vertex $\chi^2$ is chosen. MC simulations show that up to 5.1% (1.7%) of longitudinally (transversely) polarized signal events with no $\pi^0$ are misreconstructed, with one or more tracks originating from the other $B$ meson in the event. In the case of signal events with one $\pi^0$, the fraction of misreconstructed candidates is 8.8% (2.8%) for longitudinally (transversely) polarized signal events.

A neural net discriminant $\mathcal{N}$ is used in the maximum-likelihood (ML) fit, constructed from a combination of six variables calculated in the c.m. frame: the polar angles of the $B$ meson momentum vector and the $B$ meson thrust axis with respect to the beam axis, the angle between the $B$ meson thrust axis and the thrust axis of the rest of the event, the ratio of the second- and zeroth-order momentum-weighted Legendre polynomial moments of the energy flow around the $B$ meson thrust axis [17], the flavor of the other $B$ meson as reported by a multivariate tagging algorithm [18], and the boost-corrected proper-time difference between the decays of the two $B$ mesons divided by its variance. The discriminant is trained using MC for the signal, and $q\bar{q}$ continuum MC, off-resonance data and on-resonance data outside the signal region for the background.

An extended unbinned ML fit is used to extract the signal yield and polarization simultaneously for each mode. The extended likelihood function is

$$\mathcal{L} = \frac{1}{N!} \exp\Big(-\sum_j n_j\Big) \prod_{i=1}^{N} \Big[\sum_j n_j \mathcal{P}_j(\vec{x}_i; \vec{\alpha}_j)\Big]. \quad (2)$$

We define the likelihood $\mathcal{L}_i$ for each event candidate $i$ as the sum of $n_j \mathcal{P}_j(\vec{x}_i; \vec{\alpha}_j)$ over three hypotheses $j$: signal

(including misreconstructed signal candidates), $q\bar{q}$ background, and $B\bar{B}$ backgrounds as discussed below. $\mathcal{P}_j(\vec{x}_i;\vec{\alpha}_j)$ is the product of the probability density functions (PDFs) for hypothesis $j$ evaluated for the $i$-th event's measured variables $\vec{x}_i$. $n_j$ is the yield for hypothesis $j$, and $N$ is the total number of events in the sample. The quantities $\vec{\alpha}_j$ represent parameters to describe the expected distributions of the measured variables for each hypothesis $j$. Each discriminating variable $\vec{x}_i$ in the likelihood function is modeled with a PDF, where the parameters $\vec{\alpha}_j$ are extracted from MC simulation, off-resonance data, or $(m_{\rm ES}, \Delta E)$ sideband data. The seven variables $\vec{x}_i$ used in the fit are $m_{\rm ES}$, $\Delta E$, $\mathcal{N}$, and the invariant masses and cosines of the helicity angle of the two $K^*$ candidates. Since the linear correlations among the fitted input variables are found to be on average about 1%, with a maximum of 5%, we take each $\mathcal{P}_j$ to be the product of the PDFs for the separate variables.

For the signal, we use relativistic Breit-Wigner functions for the $K^{*0}$ and $K^{*\pm}$ invariant masses and a sum of two Gaussians for $m_{\rm ES}$ and $\Delta E$. The longitudinal (transverse) helicity angle distributions are described with a $\cos^2\theta$ ($\sin^2\theta$) function corrected for changes in efficiency as a function of helicity angle. The correction also accounts for the reduction in efficiency at a helicity near 0.78 introduced indirectly by the criteria used to veto $D$ mesons. The continuum $m_{\rm ES}$ shape is described by the function $x\sqrt{1-x^2}\exp[-\xi(1-x^2)]$ with $x = m_{\rm ES}/E_B^*$ and $\xi$ a free parameter [19], while second- and third-order polynomials are used for $\Delta E$ and the helicity angles, respectively. The continuum invariant mass distributions contain peaks due to real $K^*$ candidates; we model the peaking mass component using the parameters extracted from the fit to the MC signal invariant mass distributions together with a second-order polynomial to represent the nonpeaking component. The $B\bar{B}$ backgrounds use the same $m_{\rm ES}$ function as the continuum and an empirical nonparametric function [20] for all other variables. The neural net distributions are modeled using the empirical nonparametric function for all hypotheses.

$B\bar{B}$ backgrounds that remain after the event selection criteria have been applied are identified and modeled using MC simulation [21]. There are no significant charmless $B\bar{B}$ backgrounds. However, decays from higher mass $K_0^{*0}(1430)$ states are not fully simulated due to their uncertain cross section and resonance structure and we treat these as an explicit systematic uncertainty later. The charm $B\bar{B}$ backgrounds are effectively suppressed by applying the veto on the $D$ meson mass described above. No specific charm decay mode dominates the charm $B\bar{B}$ background. The charm decay modes that pass the selection are formed from the decay products of a $D$, $D^*$, or $D_s^{*\pm}$, together with another track from the event. We expect that each selected charm decay mode will contribute one or fewer events to the sample. The polarization and branching fractions of these backgrounds are uncertain and so we fix the $B\bar{B}$ background yield in the fit and then vary the yield by $\pm 100\%$ as a systematic cross-check.

We fit for the branching fraction $\mathcal{B}$ and $f_L$ simultaneously and exploit the fact that $\mathcal{B}$ is less correlated with $f_L$ than is either the yield or efficiency taken separately. The continuum background PDF parameters that are allowed to vary are $\xi$ for $m_{\rm ES}$, the slope of $\Delta E$, and the polynomial coefficients and normalizations describing the mass and helicity angle distributions. We validate the fitting procedure and obtain the sizes of potential biases on the fit results by applying the fit to ensembles of simulated experiments using the extracted fitted yields from data. The $q\bar{q}$ component is drawn from the PDF, and the signal and $B\bar{B}$ background events are randomly sampled from the fully simulated MC samples. Any observed fit bias is subtracted from the fitted yield.

The total event sample consists of 1381 and 3201 events for $B^+ \to \bar{K}^{*0}K^{*+}$ with $K^{*+} \to K_S^0\pi^+$ and $K^{*+} \to K^+\pi^0$, respectively. The results of the ML fits are summarized in Table I. We compute the branching fractions $\mathcal{B}$ by dividing the bias-corrected yield by the number of $B\bar{B}$ pairs, the reconstruction efficiency $\epsilon$ given the fitted $f_L$, and the secondary branching fractions, which we take to be 2/3 for $\mathcal{B}(\bar{K}^{*0} \to K^-\pi^+)$ and $\mathcal{B}(K^{*+} \to K^0\pi^+)$, 1/3 for $\mathcal{B}(K^{*+} \to K^+\pi^0)$, and $0.5 \times (69.20 \pm 0.05)\%$ for $\mathcal{B}(K^0 \to K_S^0 \to \pi^+\pi^-)$. The significance $S$ of the signal is defined as $S = \sqrt{2\Delta \ln\mathcal{L}}$, where $\Delta \ln\mathcal{L}$ is the change in log-likelihood from the maximum value when the number of signal events is set to zero, corrected for the systematic errors by convolving the likelihood function with a

TABLE I. Summary of results for the fitted yields, fit biases, average reconstruction efficiencies $\epsilon$ for the fitted $f_L$, sub-branching fractions $\prod \mathcal{B}_i$, longitudinal polarization $f_L$, branching fraction $\mathcal{B}$ ($B^+ \to \bar{K}^{*0}K^{*+}$), and $\mathcal{B}$ significance $S$. The first error is statistical and the second, if given, is systematic.

| Final state | $K^-\pi^+K_S^0\pi^+$ | $K^-\pi^+K^+\pi^0$ |
|---|---|---|
| Yields (events): | | |
| Total | 1381 | 3201 |
| Signal | $6.9^{+4.5}_{-3.5}$ | $13.9^{+7.6}_{-6.4}$ |
| $q\bar{q}$ background | $1365 \pm 37$ | $3169 \pm 57$ |
| $B\bar{B}$ background (fixed) | 10 | 19 |
| ML fit biases | $-0.12$ | 0.08 |
| Efficiencies and $\mathcal{B}$: | | |
| $\epsilon(\%)$ | $11.44 \pm 0.08$ | $7.40 \pm 0.08$ |
| $\prod \mathcal{B}_i(\%)$ | 15.37 | 22.22 |
| $f_L$ | $0.72^{+0.23}_{-0.36} \pm 0.03$ | $0.79^{+0.22}_{-0.36} \pm 0.03$ |
| $\mathcal{B}$ ($\times 10^{-6}$) | $0.85^{+0.61}_{-0.44} \pm 0.11$ | $1.80^{+1.01}_{-0.85} \pm 0.16$ |
| $\mathcal{B}$ Significance $S$ ($\sigma$) | 2.28 | 2.18 |
| Combined results: | | |
| $f_L$ | $0.75^{+0.16}_{-0.26} \pm 0.03$ | |
| $\mathcal{B}$ ($\times 10^{-6}$) | $1.2 \pm 0.5 \pm 0.1$ | |
| $\mathcal{B}$ Significance $S$ ($\sigma$) | 3.7 | |

Gaussian distribution with a variance equal to the total systematic error defined below. We confirm that $\sqrt{2\Delta \ln \mathcal{L}}$ is a reliable estimate of the significance $S$ by fitting ensembles of simulated experiments with background events only, using the fitted parameters and background yields from the data, and observing how often the number of fitted signal events exceeds the fitted signal yield in the data. The significance of the combined $B^+ \to \bar{K}^{*0} K^{*+}$ branching fractions is $3.7\sigma$, including statistical and systematic uncertainties.

Figs. 2 and 3 show the projections of the two fits onto $m_{\rm ES}$, $\Delta E$, and the $K^{*\pm}$ and $K^{*0}$ masses and cosines of the helicity angle for the final state with zero and one $\pi^0$, respectively. The candidates in the figures are subject to a requirement on the probability ratio $\mathcal{P}_{\rm sig}/(\mathcal{P}_{\rm sig} + \mathcal{P}_{\rm bkg})$, optimized to enhance the visibility of potential signal, where $\mathcal{P}_{\rm sig}$ and $\mathcal{P}_{\rm bkg}$ are the signal and the total background probabilities, respectively, computed without using the variable plotted. The dip in helicity at $\sim$0.78 is created by the criteria used to veto the charm background.

The systematic uncertainties on the branching fractions are summarized in Table II. The major uncertainty is the unknown background from the decays $B^+ \to K^{*+} \bar{K}_0^{*0}(1430)$ and $B^+ \to \bar{K}^{*0} K_0^{*+}(1430)$. We take the central value of the branching fraction of $B^+ \to \bar{K}_0^{*0}(1430) K^+$ [22] as an estimate of the $K_0^*(1430)$ $K^*$ branching fraction. We use the LASS parameterization for the $K_0^*(1430)$ line shape, which consists of the $K_0^*(1430)$ resonance together with an effective-range nonresonant component [23], and assume that interference effects between the $K^*$ and the spin-0 final states (nonresonant and $K_0^*(1430)$) integrate to zero as the acceptance of the detector and analysis is nearly uniform in the $K^*$ decay angles. This line shape is used to calculate the number of background events in the $K^*$ mass range. We estimate 0.81 and 0.77 events in the modes without and with a $\pi^0$, respectively.

The other errors on the branching fractions arise from the PDFs, fit biases and $B\bar{B}$ background yields, and efficiencies. The PDF uncertainties are calculated by varying

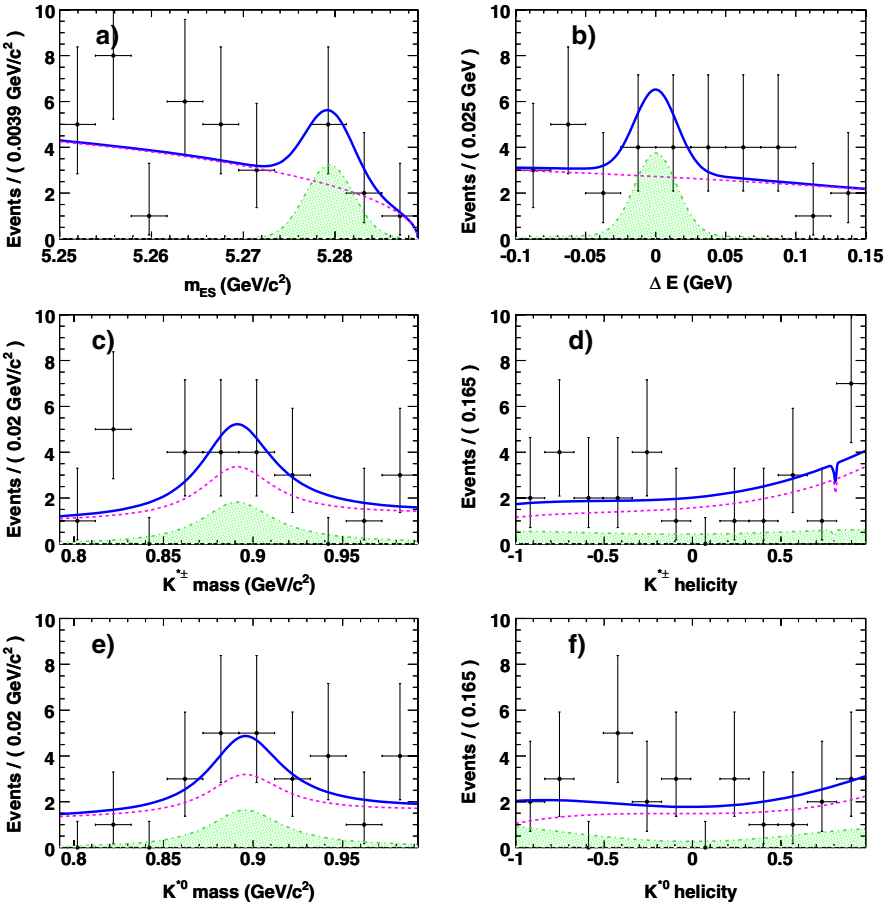


FIG. 2 (color online). Projections for $B^+ \to \bar{K}^{*0}(\to K^- \pi^+) K^{*+}(\to K_S^0 \pi^+)$ of the multidimensional fit onto (a) $m_{\rm ES}$; (b) $\Delta E$; (c) $K^{*\pm}$ mass; (d) cosine of $K^{*\pm}$ helicity angle; (e) $K^{*0}$ mass; and (f) cosine of $K^{*0}$ helicity angle for events selected with a requirement on the signal-to-total likelihood probability ratio, optimized for each variable, with the plotted variable excluded. The points with error bars show the data; the solid line shows signal-plus-background; the dashed line is the continuum background; and the hatched region is the signal.

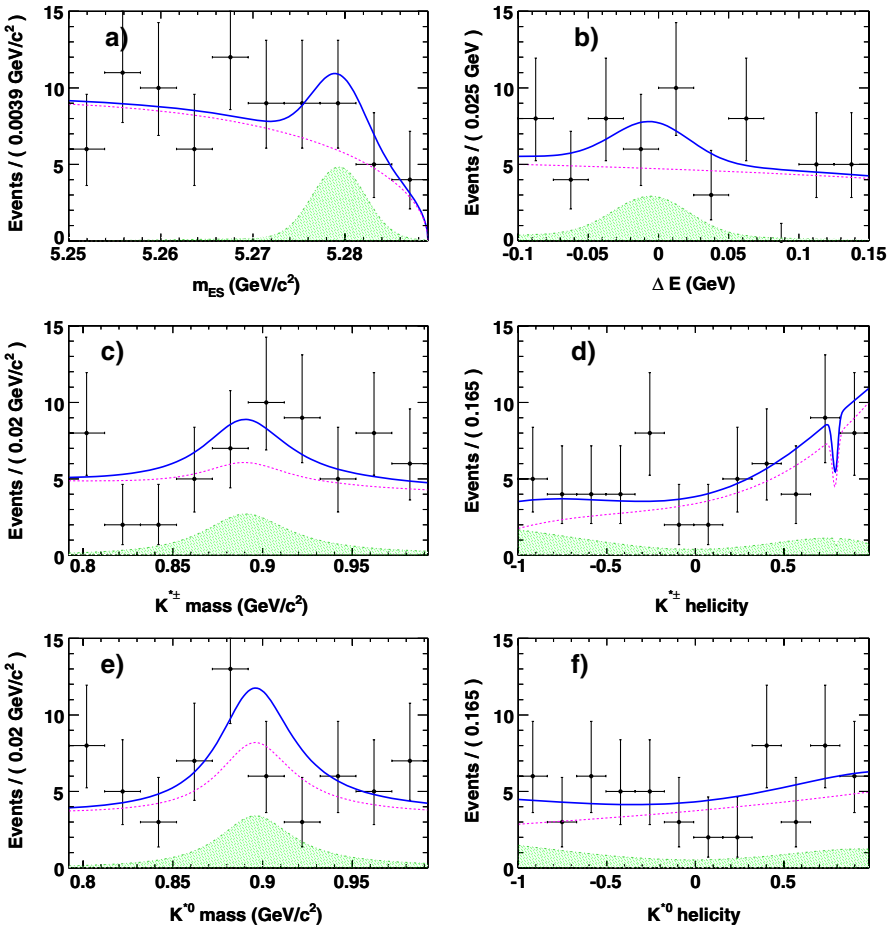


FIG. 3 (color online). Projections for $B^+ \to \bar{K}^{*0}(\to K^-\pi^+)K^{*+}(\to K^+\pi^0)$ of the multidimensional fit onto (a) $m_{\rm ES}$; (b) $\Delta E$; (c) $K^{*\pm}$ mass; (d) cosine of $K^{*\pm}$ helicity angle; (e) $K^{*0}$ mass; and (f) cosine of $K^{*0}$ helicity angle. The same projection criteria and legend are used as in Fig. 2.

TABLE II. Estimated systematic errors on the branching fraction in the final fit. Error sources which are correlated and uncorrelated when combined from the two decays are denoted by C and U, respectively.

| Final state | $K^-\pi^+K^0_S\pi^+$ | $K^-\pi^+K^+\pi^0$ |
|---|---|---|
| Additive errors (events): | | |
| Fit bias [U] | 0.08 | 0.09 |
| Fit parameters [U] | 0.10 | 0.39 |
| LASS backgrounds [U] | 0.81 | 0.77 |
| $B\bar{B}$ backgrounds [U] | 0.10 | 0.60 |
| Total additive (events) | 0.83 | 1.06 |
| Multiplicative errors (%): | | |
| Track multiplicity [C] | 1.0 | 1.0 |
| MC statistics [U] | 0.2 | 0.2 |
| Number of $B\bar{B}$ pairs [C] | 1.1 | 1.1 |
| PID [C] | 3.3 | 3.3 |
| Neutrals corrections [C] | - | 3.0 |
| $K^0_S$ corrections [C] | 1.4 | - |
| Tracking corrections [C] | 2.4 | 2.4 |
| Total multiplicative (%) | 4.2 | 4.7 |
| Total $\mathcal{B}$ error ( $\times 10^{-6}$) | 0.11 | 0.16 |

the PDF parameters that are held fixed in the original fit by their errors, taking into account correlations. The uncertainty from the fit bias includes its statistical uncertainty from the simulated experiments and half of the correction itself, added in quadrature. The uncertainties in PDF modeling and fit bias are additive in nature and affect the significance of the branching fraction results. We take a conservative approach and assume the sources of the uncertainties that contribute to the additive errors are uncorrelated when combined to form the overall $B^+ \to \bar{K}^{*0}K^{*+}$ branching fraction. Multiplicative uncertainties include reconstruction efficiency uncertainties from tracking and particle identification (PID), track multiplicity, MC signal efficiency statistics, and the number of $B\bar{B}$ pairs. The majority of the systematic uncertainties on $f_L$ cancel and the error is dominated by the uncertainty on the PDF parameters. This is calculated to be $\pm 0.03$ for both modes.

In summary, we have seen a significant excess of events and have measured the branching fraction $\mathcal{B}(B^+ \to \bar{K}^{*0}K^{*+}) = [1.2 \pm 0.5(\text{stat}) \pm 0.1(\text{syst})] \times 10^{-6}$ and the longitudinal polarization $f_L = 0.75^{+0.16}_{-0.26} \pm 0.03$. These measurements are compatible with theoretical predictions.

We are grateful for the extraordinary contributions of our PEP-II colleagues in achieving the excellent luminosity and machine conditions that have made this work possible. The success of this project also relies critically on the expertise and dedication of the computing organizations that support *BABAR*. The collaborating institutions wish to thank SLAC for its support and the kind hospitality extended to them. This work is supported by the US Department of Energy and National Science Foundation, the Natural Sciences and Engineering Research Council (Canada), the Commissariat à l'Energie Atomique and Institut National de Physique Nucléaire et de Physique des Particules (France), the Bundesministerium für Bildung und Forschung and Deutsche Forschungsgemeinschaft (Germany), the Istituto Nazionale di Fisica Nucleare (Italy), the Foundation for Fundamental Research on Matter (The Netherlands), the Research Council of Norway, the Ministry of Education and Science of the Russian Federation, Ministerio de Educación y Ciencia (Spain), and the Science and Technology Facilities Council (United Kingdom). Individuals have received support from the Marie Curie IEF program (European Union) and the A. P. Sloan Foundation.

[1] N. Cabibbo, Phys. Rev. Lett. **10**, 531 (1963); M. Kobayashi and T. Maskawa, Prog. Theor. Phys. **49**, 652 (1973).
[2] M. Beneke, J. Rohrer, and D. Yang, Nucl. Phys. **B774**, 64 (2007).
[3] H. Y. Cheng and K. C. Yang, Phys. Rev. D **78**, 094001 (2008).
[4] A. Ali *et al.*, Z. Phys. C **1**, 269 (1979); M. Suzuki, Phys. Rev. D **66**, 054018 (2002).
[5] K.-F. Chen *et al.* (Belle Collaboration), Phys. Rev. Lett. **94**, 221804 (2005); B. Aubert *et al.* (*BABAR* Collaboration), Phys. Rev. Lett. **98**, 051801 (2007); **99**, 201802 (2007).
[6] B. Aubert *et al.* (*BABAR* Collaboration), Phys. Rev. Lett. **100**, 081801 (2008).
[7] A. Kagan, Phys. Lett. B **601**, 151 (2004); C. Bauer *et al.*, Phys. Rev. D **70**, 054015 (2004); P. Colangelo *et al.*, Phys. Lett. B **597**, 291 (2004); M. Ladisa *et al.*, Phys. Rev. D **70**, 114025 (2004); H.-n. Li and S. Mishima, Phys. Rev. D **71**, 054025 (2005); M. Beneke *et al.*, Phys. Rev. Lett. **96**, 141801 (2006).
[8] A. Datta *et al.*, Phys. Rev. D **76**, 034015 (2007).
[9] B. Aubert *et al.* (*BABAR* Collaboration), Phys. Rev. D **78**, 051103 (2008).
[10] R. Godang *et al.* (CLEO Collaboration), Phys. Rev. Lett. **88**, 021802 (2001).
[11] Charge-conjugate decays are implicitly included.
[12] B. Aubert *et al.* (*BABAR* Collaboration), Nucl. Instrum. Methods Phys. Res., Sect. A **479**, 1 (2002).
[13] G. Kramer and W. F. Palmer, Phys. Rev. D **45**, 193 (1992).
[14] W.-M. Yao *et al.* (Particle Data Group), J. Phys. G **33**, 1 (2006).
[15] B. Aubert *et al.* (BABAR Collaboration), Phys. Rev. D **66**, 032003 (2002).
[16] S. Brandt *et al.*, Phys. Lett. **12**, 57 (1964); E. Farhi, Phys. Rev. Lett. **39**, 1587 (1977).
[17] B. Aubert *et al.* (*BABAR* Collaboration), Phys. Rev. D **70**, 032006 (2004).
[18] B. Aubert *et al.* (*BABAR* Collaboration), Phys. Rev. Lett. **94**, 161803 (2005).
[19] H. Albrecht *et al.* (ARGUS Collaboration), Phys. Lett. B **241**, 278 (1990).
[20] K. S. Kramer, Comput. Phys. Commun. **136**, 198 (2001).
[21] S. Agostinelli *et al.* (GEANT Collaboration), Nucl. Instrum. Methods Phys. Res., Sect. A **506**, 250 (2003).
[22] B. Aubert *et al.* (*BABAR* Collaboration), Phys. Rev. D **76**, 071103 (2007).
[23] D. Aston *et al.* (LASS Collaboration), Nucl. Phys. **B296**, 493 (1988).